6R Instrumented Spatial Linkages for Anatomical Joint Motion Measurement—Part 2: Calibration

S. J. Kirstukas

J. L. Lewis

Departments of Mechanical Engineering and
Orthopaedic Surgery,
University of Minnesota,
Minneapolis, MN 55455

A. G. Erdman

Department of Mechanical Engineering,
University of Minnesota,
Minneapolis, MN 55455

The six-revolute-joint instrumented spatial linkage (6R ISL) is often the measurement system of choice for monitoring motion of anatomical joints. However, due to tolerances of the linkage parameters, the system may not be as accurate as desired. A calibration algorithm and associated calibration device have been developed to refine the initial measurements of the ISL's mechanical and electrical parameters so that the measurement of six-degree-of-freedom motion will be most accurate within the workspace of the anatomical joint. The algorithm adjusts the magnitudes of selected linkage parameters to reduce the squared differences between the six known and calculated anatomical position parameters at all the calibration positions. Weighting is permitted so as to obtain a linkage parameter set that is specialized for measuring certain anatomical position parameters. Output of the algorithm includes estimates of the measuring system accuracy. For a particular knee-motion-measuring ISL and calibration device, several interdependent design parameter relationships have been identified. These interdependent relationships are due to the configuration of the ISL and calibration device, the number of calibration positions, and the limited resolution of the devices that monitor the position of the linkage joints. It is shown that if interdependence is not eliminated, then the resulting ISL parameter set will not be accurate in measuring motion outside of the calibration positions, even though these positions are within the ISL workspace.

Introduction

As with any measuring system, an instrumented spatial linkage (ISL) must be tested and calibrated before it can be used with confidence. This paper details the calibration technique developed for improving the measurement resolution of a 6R ISL—a serial ISL design where the links are interconnected by six revolute joints.

With a 6R ISL, determination of anatomical joint position is based upon a mathematical function that approximates what is actually occurring with the physical model. The independent variables of this function are six voltages, each relating to a different linkage joint angle; the dependent variables are the six anatomical position parameters. In measuring the anatomical joint position of one bony coordinate frame relative to the other, this function contains twenty-four fixed mechanical parameters and generally twelve additional fixed electrical parameters that relate linkage joint angles to the voltages output by the devices that monitor the linkage joints, typically potentiometers [5]. The function does not take into account several documented error sources, such as rotational and translational clearances of the linkage joints or potentiometer voltage variability due to temperature fluxuations, electrical interference, or hysteresis [3,8].

The presumed mechanical parameters of an ISL may differ from the actual parameters due to either inevitable tolerance and construction errors or bending of linkage components from rough handling. We have found that these fixed mechanical tolerance errors can be on the order of several millimeters or degrees. Small errors in individual linkage parameters can have a large effect in the calculation of position and displacement data [4].

The goal of the calibration procedure is to adjust the nominal mechanical and electrical parameters of the ISL to optimize the accuracy of the ISL within the calibration space. Although tolerances of the electrical devices are variable and cannot be completely calibrated out, Sommer and Miller [7] have demonstrated that the adjustment of the mechanical and electrical parameters can greatly improve positional measurement accuracy. They used a Levenberg-Marquardt algorithm to refine typically nineteen of the fixed ISL parameters. Their algorithm attempted to minimize the squared difference between known and calculated sets of three Euler angles and three orthogonal translations that related one linkage end to the other. The objective function was nonweighted and used centimeters and radians as the units in measuring translation and rotation, respectively. The value of this procedure depends on the accuracy and range of the "known" calibration data.

Most calibration devices referenced in the literature [3, 7] allow only a few degrees of freedom. None of these calibration

devices appear to allow calibration of the linkage in the same workspace in which it will be used. This paper discusses the requirements of a general calibration scheme and outlines a method and associated hardware used for calibrating an ISL in a particular workspace. The new calibration device can replicate four of the six anatomical position parameters, effectively allowing the ISL to be calibrated for the very motion it will measure. By calibrating the ISL in the anatomical space in which it will be used, the refined parameter set can compensate for various error sources to some degree. The calibration algorithm utilizes the six anatomical position parameters in the objective function and has the capability to increase the accuracy of specific anatomical position parameters with the use of weighting factors. Additionally, the mean residuals output by the algorithm provide an estimate for the accuracy of the ISL in the measurement of the total six-degree-of-freedom (6-DOF) position data for the joint.

Background

Of the twenty-four fixed mechanical ISL parameters (refer to the companion paper [5] for complete definitions of the ISL parameters), ten parameters are dependent upon ISL attachment to the anatomical joint, while fourteen parameters are constant regardless of attachment site. Because the ten external ISL parameters are incorporated into transformations that locate the bony coordinate frames relative to the linkage ends, the calibration scheme is primarily concerned with the refinement of the fourteen internal mechanical parameters—a_2, s_2, α_2 through a_6—and the twelve electrical ISL parameters—θslope$_1$ and θzero$_1$ through θslope$_6$ and θzero$_6$; θslope$_i$ and θzero$_i$ are the coefficients of the approximately linear relationship between the ith linkage joint angle and the ith potentiometer output voltage:

$$\theta_i = \theta\text{slope}_i(v_i) + \theta\text{zero}_i \qquad (1)$$

where:
v_i is the voltage output of the ith potentiometer.

For ISLs used in the laboratory, it is convenient to mount machined steel cross hairs, representing the x- and y-axes of the end coordinate frames, on the shafts of revolute axes 1 and 6. The two sets of cross hairs indicate end coordinate frames from which the bony coordinate frames are referenced. A general ISL design can be modelled between the two end frames by using six sets of Denavit-Hartenberg parameters. Each set of parameters (a_i, s_i, α_i and θ_i) is assembled together in a joint transformation matrix $\mathbf{A}_1$ [5], and the total end-to-end transformation matrix, $\mathbf{H}_{\text{ISL}}$, can be constructed between the moving and stationary end coordinate frames by multiplying the six $\mathbf{A}_i$ matrices together as follows:

$$\mathbf{H}_{\text{ISL}} = \mathbf{A}_6 \, \mathbf{A}_5 \, \mathbf{A}_4 \, \mathbf{A}_3 \, \mathbf{A}_2 \, \mathbf{A}_1 \qquad (2)$$

Note that the calculation of $\mathbf{H}_{\text{ISL}}$ includes six joint coordinate transformations. As such, external ISL parameters a_1, s_1, α_1 and s_6 are included in Eq. (2) in addition to the fourteen fixed internal mechanical parameters and twelve fixed electrical parameters, making $\mathbf{H}_{\text{ISL}}$ a function of thirty fixed parameters and six voltages.

The purpose of linkage calibration is to adjust the nominal mechanical and electrical ISL parameters so that the anatomical position parameters within a prescribed workspace is done with a minimum of error. Typically, the calibration procedure involves two parts—data sampling and ISL parameter refinement. Generally, some sort of calibration device places the ISL in a finite number of known relative positions. At each calibration position, the six known position parameters and the voltages from the six monitored linkage joints are recorded. From the experimental data and the current set of estimated linkage parameters, a transformation matrix is constructed and predicted position components are calculated using the method
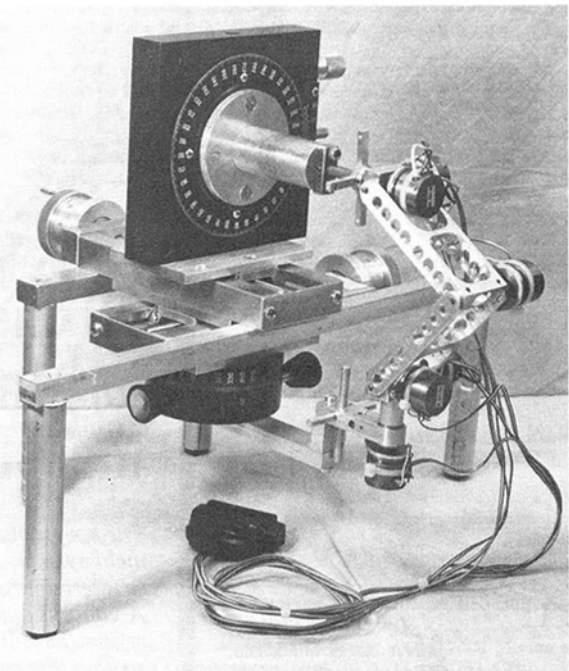

Fig. 1 A photograph of the ISL mounted on the calibration device. The calibration device is capable of simulating a positive and negative range of four of the six possible anatomical position parameters: flexion, lateral translation, anterior drawer, and tibial rotation.

developed by Grood and Sutay [2]. The differences between the six predicted and the six known position components are the position residuals. A regression algorithm refines the ISL parameters to minimize these residuals.

Methods

To accurately measure anatomical motion, the ISL must be calibrated over the entire anatomical joint workspace. A calibration device that can reproduce four of the six anatomical displacements has been developed to aid in the calibration of a knee motion-measuring ISL (Fig. 1). The ISL can be mounted laterally on the device to obtain a similar attachment as is used during motion measurement of human knee joints. The ISL attaches to the calibration device (or hardware attached to an anatomical joint) by just two screws. The attachment sites are secure and repeatable due to the presence of male and female mating surfaces.

The calibration device is a four-DOF mechanism containing two prismatic joints and two revolute joints. The mechanism joints are aligned in such a way that the mechanism's rotations (R_1 and R_2) and translations (T_1 and T_2) correspond exactly to the anatomical position parameters as defined by Grood and Suntay [2] for flexion/extension, tibial rotation, medial/lateral translation, and anterior/posterior drawer, respectively. The remaining two position parameters—joint compression/distraction and abduction/adduction—cannot be reproduced by the device and are fixed at zero. The variable calibration device parameters are read directly from the dials and have a resolution of 0.01 millimeter for the two prismatic joints and 1/60th of a degree for the two revolute joints. Due to the design of the calibration device, when the device is set at representative knee positions the ISL will form configurations that will be assumed during actual use.

For the calibration device, the relative position of one ISL attachment site to the other is modelled as a ten-parameter function dependent on the four calibration device settings (R_1, R_2, T_1, and T_2), and five fixed linear parameters and one fixed angular parameter—as labeled in Fig. 2. The five parameters,
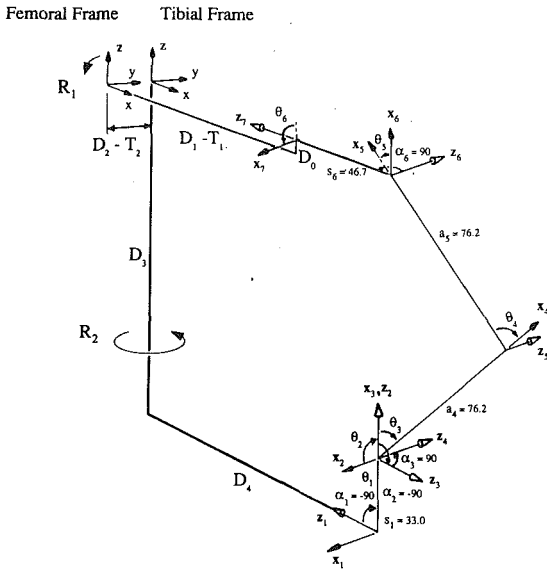
Fig. 2 Schematic of the ISL mounted on the calibration device, illustrating the parameters of the calibration device and ISL. Internal to the device, two coordinate frames are defined from which the anatomical position parameters are referenced. These coordinate frames are aligned the same as the bony coordinate frames; with the z-axis superior and the y-axis anterior. In the configuration shown, the calibration device's tibial coordinate frame is positioned in anterior drawer by an amount equal to $D_2 - T_2$.
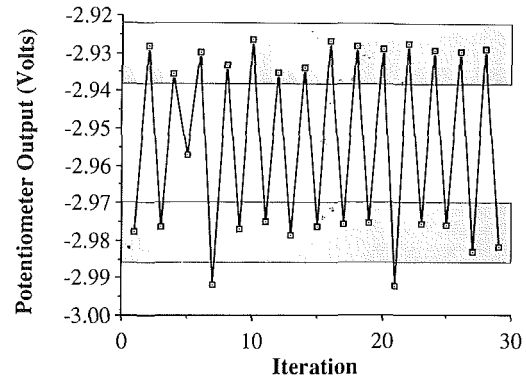

Fig. 3 Oscillating voltage outputs demonstrate hysteresis of potentiometer 1 (the potentiometer mounted closest to the tibia) as the calibration device variable that simulates tibial rotation was repeatedly reset at zero from alternating directions. Scatter within bands is largely attributable to potentiometer variability and human error in precisely locating the zero position.

D_0, D_1, D_2, D_3 and D_4 are the link lengths of the calibration device. Parameter ψ, left off the figure for the sake of clarity, is the angular amount that the lever arm, indicated by D_0, deviates from a plane perpendicular to the axis of flexion, indicated by $D_1 - T_1$.

The refinement of the ISL parameters can be approached as the minimization of an objective function. The objective function measures the squared difference between the six known position parameters and the six position parameters extracted from the transformation matrix that is calculated using the current estimates for the thirty fixed ISL parameters together with the six potentiometer voltage outputs corresponding to each of the n number of calibration positions. Use of the extracted position parameters in the objective function offers the capability to independently weight the six position parameters, enabling an ISL to be tuned to measure certain anatomical position parameters more sensitively.

However, the position parameters cannot be directly extracted from the end-to-end transformation matrix H_{ISL} if they are to have any real correlation with anatomical parameters. The anatomical position parameters must be taken from an equivalent bone-to-bone transformation matrix. If PRE is a transformation matrix that links the proximal ISL end coordinate frame to the calibration device's simulated femoral bone coordinate system, and if POST links the calibration device's simulated tibial bone coordinate system with the distal ISL end coordinate frame, then the position parameters should be extracted from matrix H, where H is defined:

$$H = [PRE][H_{ISL}][POST]. \qquad (3)$$

The components of matrices PRE and POST relate directly to the geometry of the calibration device. All fixed calibration device parameters except D_2 participate in the calculation of PRE and POST. Device parameter D_2 is not included because of the manner in which the anatomical position parameters are defined; instead it will later be incorporated into the calculation of known anterior drawer.

For the calibration device shown in Fig. 3, PRE and POST are:

$$PRE = \begin{bmatrix} 0 & -\sin\psi & -\cos\psi & D_1 - D_0\sin\psi \\ -1 & 0 & 0 & 0 \\ 0 & \cos\psi & -\sin\psi & D_0\cos\psi \\ 0 & 0 & 0 & 1 \end{bmatrix} \qquad (4a)$$

$$POST = \begin{bmatrix} 0 & -1 & 0 & 0 \\ 0 & 0 & 1 & D_3 \\ -1 & 0 & 0 & D_4 \\ 0 & 0 & 0 & 1 \end{bmatrix} \qquad (4b)$$

The calibration objective function evaluates the weighted squared difference between set of known position parameters (as read from the calibration device) and set of calculated position parameters The function is expressed mathematically as:

$$F(\mathbf{x}) = \sum_{i=1}^{n} \sum_{j=1}^{6} w_j(KP_{ij} - P_{ij}(\mathbf{x}, v_i))^2 \qquad (5)$$

where:

KP_{ij} = the jth known position parameter at the ith calibration position; the four nonzero position parameters are read from the calibration device

P_{ij} = the jth position parameter at the ith calibration position, extracted from H, which was calculated using the current set of estimates for the thirty mechanical and electrical ISL parameters and the six calibration device parameters

$\mathbf{x}$ = the vector of adjustable mechanical and electrical parameters

v_i = the vector of six potentiometer voltages corresponding to the ith calibration position

w_j = the set of six weight factors, one corresponding to each of the position parameters

n = the number of calibration positions

The following equations show how the variable calibration device parameters (R_1, R_2, T_1, and T_2) and the fixed calibration device parameter D_2 are incorporated into the calculation of the six differences between known and calculated position parameters at the ith calibration position for use in Eq. 5:

$$KP_{i1} - P_{i1} = R_1 - FLX \qquad (6a)$$

$$KP_{i2} - P_{i2} = 0 - ABD \qquad (6b)$$

$$KP_{i3} - P_{i3} = -R_2 - ER \qquad (6c)$$

$$KP_{i4} - P_{i4} = T_1 - LT \qquad (6d)$$

$$KP_{i5} - P_{i5} = (D_2 - T_2) - AD \qquad (6e)$$

$$KP_{i6} - P_{i6} = 0 - JD \qquad (6f)$$

where:

FLX, ABD, ER, LT, AD, JD are the calculated magnitudes of the position parameters flexion, abduction, external rotation, lateral translation, anterior drawer, joint distraction, respectively

Mean position residuals, the normalized difference between the predicted and measured position parameters, are commonly used to estimate the measurement error present with ISL use. The mean residual corresponding to the jth position parameter is calculated as the square root of the nonweighted average of squared differences [7]:

$$\sigma_j = \left(\frac{1}{\mathbf{n}} \sum_{i=1}^{n} (KP_{ij} - P_{ij})^2 \right)^{1/2} \qquad (7)$$

where:

σ_j = the mean residual corresponding to the jth position parameter

A Levenberg-Marquardt least-squares algorithm can be used to minimize the nonlinear calibration objective function $[F(\mathbf{x}),$ Eq. (5)] by altering ISL parameters. The Levenberg-Marquardt method is a variation of the Gauss-Newton method, the simplest algorithm for small residual nonlinear regression problems. Close to the solution, the algorithm behaves as the Gauss-Newton method and offers superlinear convergence. When further from the solution, a method similar to a steepest descent method is employed. The Levenberg-Marquardt method is particularly effective for problems in which the objective function is capable of approaching zero. This method has been successfully used for linkage calibration [7].

The Levenberg-Marquardt optimization scheme requires the computation of a Jacobian matrix of partial derivatives. The entries of the Jacobian are the partial derivatives of the six position parameters with respect to the adjustable ISL parameters for the n positions:

$$\left.\begin{array}{l} \text{for } i = 1 \ldots \mathbf{n} \\ \text{for } j = 1 \ldots 6 \\ \text{and } k = 1 \ldots 30 \end{array}\right\} \quad J_{(6(i-1)+j),k} = \frac{\partial P_{ij}}{\partial x_k} \qquad (8)$$

where:

$J_{(6(i-1)+j),k}$ = the entries of the Jacobian matrix of partial derivatives

P_{ij} = the jth position parameter, calculated using the current set of estimates for the thirty mechanical and electrical parameters at the ith calibration position

x_k = the kth ISL parameter

Each column of the Jacobian matrix corresponds to an ISL parameter that will be refined. ISL parameters that can be accurately determined will be held fixed and will not participate in the Jacobian. Each row of the Jacobian corresponds to one of the six position parameters at a calibration position. Therefore, the Jacobian matrix will have $6n$ rows and as many as thirty columns. Because calculation of the partial derivatives of the position parameters is dependent on the matrix entries of $\mathbf{H}$, which are in turn functions of the thirty ISL parameters, the calculation of the Jacobian matrix requires use of the

derivative chain rule. The computation of the partial derivatives of $\mathbf{H}$ with respect to the thirty ISL parameters is demonstrated in Appendix 1. Letting $\mathbf{D}$ represent the partial derivative of $\mathbf{H}$ with respect to an arbitrary ISL parameter, x_k, and d_{pq} represent the component of $\mathbf{D}$ occupying the pth row and qth column, the partial derivatives of the position parameters are:

$$\frac{\partial \gamma}{\partial x_k} = \left(\frac{h_{11} d_{12} - h_{12} d_{11}}{h_{11} h_{11} + h_{12} h_{12}} \right) \qquad (9a)$$

Letting, $F = h_{31} s\gamma - h_{32} c\gamma$ and $G = -h_{21} s\gamma + h_{22} c\gamma$ then,

$$\frac{\partial \alpha}{\partial x_k} = \frac{G\left(d_{31} s\gamma - d_{32} c\gamma + \left(\frac{\partial \gamma}{\partial x_k}\right) (h_{31} c\gamma + h_{32} s\gamma)\right) - F\left(-d_{21} s\gamma + d_{22} c\gamma - \left(\frac{\partial \gamma}{\partial x_k}\right) (h_{21} c\gamma + h_{22} s\gamma)\right)}{F^2 + G^2} \qquad (9b)$$

Letting, $U = h_{11} c\gamma + h_{12} s\gamma$ and $V = h_{13}$ then,

$$\frac{\partial \beta}{\partial x_k} = \frac{V\left(d_{11} c\gamma + d_{12} s\gamma - \left(\frac{\partial \gamma}{\partial x_k}\right) (h_{11} s\gamma - h_{12} c\gamma)\right) - U(d_{13})}{U^2 + V^2} \qquad (9c)$$

$$\frac{\partial(LT)}{\partial x_k} = d_{14} \qquad (9d)$$

$$\frac{\partial(AD)}{\partial x_k} = d_{24} c\alpha - h_{24}\left(\frac{\partial \alpha}{\partial x_k}\right) s\alpha - d_{34} s\alpha - h_{34}\left(\frac{\partial \alpha}{\partial x_k}\right) c\alpha \qquad (9e)$$

$$\frac{\partial(JD)}{\partial x_k} = -h_{13} d_{14} - d_{13} h_{14} - h_{23} d_{24} - d_{23} h_{24} - h_{33} d_{34} - d_{33} h_{34} \qquad (9f)$$

where:

the prefixes s and c represent sine and cosine, respectively.

$$\frac{\partial \alpha}{\partial x_k}, \frac{\partial \beta}{\partial x_k}, \frac{\partial \gamma}{\partial x_k}, \frac{\partial(LT)}{\partial x_k}, \frac{\partial(AD)}{\partial x_k}, \frac{\partial(JD)}{\partial x_k}$$

are the partial derivatives of right knee position parameters flexion, abduction, external rotation, lateral translation, anterior drawer, and joint distraction, respectively, with respect to ISL parameter x_k.

Using information supplied by the Jacobian matrix of first partial derivatives, the variable parameters are adjusted in accordance with the Levenberg-Marquardt algorithm to further minimize the objective function. Termination of the algorithm comes when no further minimization is possible or a maximum number of iterations has been exceeded. The Levenberg-Marquardt algorithm is included in Appendix 2.

The calibration algorithm was translated into a FORTRAN computer program. The units of measure used in the computer program form of the objective function are millimeters for length related position parameters and radians for angle-related position parameters. Since the magnitude of the differences in linear measurements tend to be much larger than the magnitude of differences in angular measurements, weighting is needed to bring the rotational parameters up to the level of importance of the linear parameters. If the measurement of one degree is deemed as important as the measurement of one millimeter, then a logical weighting factor would be the square of $180/\pi$, or roughly 3000.

Evaluation of the Calibration Procedure

The measurements of the six fixed parameters of the calibration device are likely to contain some error and these may be fine-tuned as well. In this way, it is possible to calibrate the calibration device as well as the ISL. However, due to several dependent relationships between the ISL and calibra-

tion device parameters, certain of the total thirty-six parameters must be held fixed. In general, when two parameter axes are parallel for all calibration positions, the affected parameters cannot be uniquely optimized. A schematic diagram of the ISL and calibration device (such as Fig. 2) is helpful in identifying the dependent relationships. From Fig. 2, it is obvious that s_6 and D_1 are both aligned in the same direction for any configuration of the calibration device. If one of these parameters is not held fixed, then there will be an infinite number of solution combinations for the set involving s_6 and D_1. Further analysis of Fig. 2 reveals two additional dependent relationships. It is evident that calibration device parameter D_3 and ISL parameter s_1 remain parallel for any position of the ISL. Likewise, nominally zero ISL parameters s_3, s_4, and s_5 are oriented along axes z_4, z_5, and z_6 and are parallel always. These three relationships require that five parameters be held fixed to achieve a nonsingular solution. We chose to hold ISL parameters s_3 and s_5 and calibration device parameters D_1 and D_3 fixed during the optimization process, leaving a total of 32 parameters that may be refined.

To test the optimization algorithm, artificial voltage data were generated for our ISL. Because there must be more data points (the six anatomical position parameters at the n calibration positions) than unknowns (as many as thirty-two ISL and calibration device parameters), six distinct positions of the ISL on the calibration device theoretically provide enough experimental data to allow a nonsingular solution and refine all parameters. However, Sommer and Miller [7] have found that using considerably more positions diminishes the effect of potentiometer variability.

In order to span the entire knee workspace, we selected forty-eight calibration positions. The positions consisted of permutations of flexion angle 0, 30, 60, and 90 degrees, lateral translation of 25 and −25 millimeters, anterior drawer of 25 and −25 millimeters, and external rotation of 30, 0, and −30 degrees. Using an inverse kinematics algorithm, the joint angles of the ISL were solved for at each of the forty-eight calibration positions. The solution sets of joint angles were then developed into a list of voltages by using typical values for θzero and θslope parameters. These forty-eight sets of theoretically derived voltages are used as input data for the calibration program.

Several calibrations were performed and the results identified several more interdependent parameter relationships. Because certain parameter axes were near-parallel for most of the calibration positions, locating a unique parameter set was not always possible. For example, a relationship exists between ISL parameters a_3 and a_6, as these parameters are located along two axes (x_3 and x_6) that are nearly parallel for many calibration positions. Additionally, ISL parameter s_2 (along axis z_3) was found to interfere with the solution of s_6 and calibration device parameter D_2 was found to be dependent upon the solution of ISL parameter a_2 (along axis x_2). To eliminate these secondary relationships, we chose to hold parameters a_6, s_2, and D_2 fixed during calibration. The interdependence of these parameters depends on the specific design of the ISL and calibration. The interdependence of these parameters depends on the specific design of the ISL and calibration device, the degrees of freedom permitted by the calibration device, and the calibration configurations. Although we have not rigorously evaluated other ISL's and calibration devices, we suspect this can occur whenever the optimization method of calibration is used. Later we will show that this phenomenon can cause large errors in ISL output.

With the four ISL parameters a_6, s_2, s_3, and s_5 held fixed along with the three calibration device parameters D_1, D_2, and D_3, the parameters optimization was successful even when the starting values of the remaining twenty-nine parameters were erroneous by two units (millimeters, degrees, or degrees/volt, as appropriate).

Satisfied that the calibration scheme was worthwhile, we tested the method with actual voltage data. To reduce the number of parameters that require refinement, the six calibration device parameters were carefully measured by mechanical means and held fixed during calibration. Table 1 shows the initial and final ISL parameter sets for several runs of the optimization program with the rotational parameters weighted at 3000. The input data set corresponds to eighty-one calibration positions consisting of permutations of flexion angle, 0, 45, and 90 degrees, lateral translation of 20, 0, and −20 millimeters, anterior drawer of 20, 0, and −20 millimeters, and external rotation of 25, 0, and −25 degrees. Column A lists the nominal ISL parameters and set of initial mean residuals. The initial set of eighteen mechanical parameters (a_i, s_i, and α_i) is expected to be rather accurate but the initial set of twelve electrical parameters represents rough estimates.

Column B shows the optimized parameters when the minimum four ISL parameters (a_6, s_2, s_3, and s_5) were held fixed. Convergence occurred in four iterations and the mean residuals are good considering the large calibration volume. However, certain members of the set of optimized ISL parameters (particularly a_3, a_4, a_5, θslope$_3$, and θslope$_4$, θslope$_5$) have assumed values drastically different than those measured directly. This is apparently an additional interdependent relationship that was able to be eliminated by holding one of the members of the interdependent set fixed. Column C shows the optimized parameters when ISL parameter a_3 is held fixed at its nominal measurement of zero millimeters. The resulting parameter set indicates that all interdependent relationships among ISL parameters and calibration parameters have been eliminated. Column D shows the optimized parameters when all nominal linear parameters equal to zero millimeters were held fixed. Examining the results of the three calibrations, it is seen that the optimized parameter set of column B yields slightly better residuals than the other two runs; however, the optimized parameters of run B are quite different from those of the actual linkage, while runs C and D produced ISL parameter sets that are very close to those actually observed. Although the optimized ISL parameter set described in column B best fits the 81 known calibration positions, the effect of this parameter set for positions outside the calibration range is unknown.

The appearance of the additional interdependence involving ISL parameter a_3 is apparently due to inadequate voltage data. Electrical noise, potentiometer hysteresis and nonlinearity, and mechanical joint clearances all contribute to the corruption of the voltage data. The scatter in the data produces an objective function surface where the correct determination of ISL parameter a_3 becomes impossible.

The linkage joints of our ISL are monitored using wirewound precision potentiometers (Maury Corporation, 10 kΩ, single turn, no stops). Among potentiometers, the magnitude of the θslopes vary slightly, with the average nominal value being 64 degrees/V. To improve potentiometer resolution during testing, the potentiometer slopes are decreased by increasing the amplifier gains as high as possible while confining voltages within the range of −10 to 10 V for any anticipated position of the ISL. A lower θslope decreases the usable range of motion for a potentiometer but allows for more accurate determination of θ within the range.

To determine the magnitude of potentiometer voltage error, tests were conducted on the assembled ISL. Collection of single voltage sets from the ISL in a stationary position yielded a standard deviation of less than 3×10^{-3} V. An increase in resolution was attained by gathering several voltage sets and using the average set as the representative set. Variability tests conducted using 100 averaged voltage sets over a three-second time span yielded a standard deviation of less than 3×10^{-4} Volts, a ten-fold decrease as anticipated by statistical theory.

However, the error due to electrical noise was found to be insignificant when compared to that caused by the other error

Table 1 Actual ISL calibration results demonstrate parameter interdependence. ISL parameters in columns B, C, and D accurate to only one digit after the decimal point have been held fixed

ISL Parameters		Initial parameter set A	Resultant ISL parameter sets ($n=81$) B	C	D
a_1	(mm)	0.0	-0.831	-0.497	0.0
a_2	(mm)	0.0	0.168	-0.174	0.0
a_3	(mm)	0.0	-29.934	0.0	0.0
a_4	(mm)	76.2	96.298	76.211	76.256
a_5	(mm)	76.2	97.051	75.829	75.877
a_6	(mm)	0.0	0.0	0.0	0.0
s_1	(mm)	33.0	34.378	34.033	34.069
s_2	(mm)	0.0	0.0	0.0	0.0
s_3	(mm)	0.0	0.0	0.0	0.0
s_4	(mm)	0.0	-3.630	-4.137	0.0
s_5	(mm)	0.0	0.0	0.0	0.0
s_6	(mm)	46.7	44.545	45.726	45.752
α_1	(deg)	-90.0	-90.896	-90.917	-90.883
α_2	(deg)	-90.0	-88.892	-88.874	-88.895
α_3	(deg)	90.0	90.091	90.164	89.992
α_4	(deg)	0.0	0.419	0.365	0.354
α_5	(deg)	0.0	0.009	-0.029	-0.679
α_6	(deg)	90.0	90.373	90.492	91.332
$\theta zero_1$	(deg)	-2.3	-3.499	-3.644	-3.832
$\theta zero_2$	(deg)	-108.9	-110.334	-110.430	-108.620
$\theta zero_3$	(deg)	6.3	8.621	-0.763	-0.679
$\theta zero_4$	(deg)	-13.2	-37.659	-23.541	-23.602
$\theta zero_5$	(deg)	16.0	28.467	23.953	23.975
$\theta zero_6$	(deg)	169.0	170.504	170.394	172.625
$\theta slope_1$	(deg/V)	64.7	61.360	61.399	61.436
$\theta slope_2$	(deg/V)	64.7	63.371	63.281	63.250
$\theta slope_3$	(deg/V)	64.7	53.276	67.238	67.211
$\theta slope_4$	(deg/V)	-71.0	-50.000	-63.460	-63.429
$\theta slope_5$	(deg/V)	-71.0	-54.295	-68.240	-68.220
$\theta slope_6$	(deg/V)	71.0	68.028	67.990	67.986
# of iterations to convergence		—	4	3	3
Mean Residuals					
flexion (deg)		1.884	0.490	0.492	0.512
abduction (deg)		1.880	0.312	0.356	0.380
tibial rotation (deg)		1.460	1.008	1.019	1.020
lateral translation (mm)		11.888	0.649	0.577	0.581
anterior drawer (mm)		3.834	0.667	0.676	0.696
joint distraction (mm)		5.223	0.875	0.984	0.981

sources. Hysteresis of the potentiometers and the mechanical linkage joints was simultaneously measured by (i) recording voltage data from the ISL in one position on the calibration device, (ii) changing one of the device variables in one direction and returning to the original position for voltage sampling, and (iii) changing the same device variable in the opposite direction and returning to the original position for voltage sampling. When steps (ii) and (iii) are repeated multiple times, a directionally dependent phenomenon is apparent. The collected voltages tend to lie in a two parallel bands rather than in a normal distribution. Figure 3 illustrates hysteresis of revolute joint 1 (the linkage joint located closest to the tibia) as the calibration device setting that controlled tibial rotation was repeatedly reset from both directions. The mean voltage of the test was found to differ by as much as 2.5×10^{-2} V from the high and low range of measured values.

A combined study of potentiometer hysteresis and linearity was accomplished by recording voltage data from the ISL at various positions of pure flexion on the calibration device. This dial was altered in twenty-degree increments ranging from -110 to 110 degrees. Four trials were conducted: two starting from a dial setting of -110 degrees and progressing positive, and two starting from $+110$ degrees and progressing negative. Because displacement of the devices's flexion dial produces only rotation of revolute joint 6, it is the voltages of potentiometer 6 that were studied.

In each of the trials, a strong linear relationship between angle and potentiometer voltage was evident; the linear regression coefficient was 1.000 for all four lines. Each set of two lines corresponding to the same direction were essentially the same: the zeroes differed by less than 2×10^{-3} V and the slopes differed from one another by less than 0.1 percent. The largest difference between measured voltages and linearly predicted voltages was less than 1×10^{-2} V. Hysteresis produced a 1.5×10^{-2} V shift between the lines corresponding to the two directions of flexion.

In considering the combined effects of electrical noise, hysteresis, nonlinearity, and mechanical joint clearances, the error in determining the true voltage is estimated as large as 3×10^{-2} Volts. This translates to a resolution of ± 0.25 degrees for potentiometers amplified at 8 degrees/V (as most of those are during our in vitro knee testing). For potentiometers at a lower gain, a resolution of ± 0.5 degrees is expected.

To determine the effect of using ISL parameter sets that produce low residuals in the calibration procedure but bear little or no resemblance to the physically observed parameter set (as in run B of Table 1), a calibration was simulated within the computer. The same artificial voltage data file developed to test the calibration scheme was rounded off to one digit after the decimal point. This corresponds to a random voltage error of $\pm 5 \times 10^{-2}$ V, an error of the same magnitude that we found present in actual voltage data. Table 2 shows the output parameter sets from three calibrations with the rotational position parameters weighted at 3000. For all calibrations, the adjustable parameters were initially made incorrect by two units—by degrees, degrees/V, or millimeters, as applicable.

Table 2 ISL calibration results for simulated data. Those ISL parameters and calibration device parameters in columns B, C, and D accurate to only one digit after the decimal point have been held fixed.

| | | True parameter set | Resultant ISL parameter sets | | |
		A	B	C	D
ISL Parameters					
a_1	(mm)	0.0	−0.014	−0.004	−0.004
a_2	(mm)	0.0	0.000	−0.001	−0.001
a_3	(mm)	0.0	−37.675	0.0	0.0
a_4	(mm)	76.2	97.155	75.158	76.029
a_5	(mm)	76.2	101.446	76.957	78.064
a_6	(mm)	0.0	0.0	0.0	0.0
s_1	(mm)	33.0	34.407	32.505	31.326
s_2	(mm)	0.0	0.0	0.0	0.0
s_3	(mm)	0.0	0.0	0.0	0.0
s_4	(mm)	0.0	0.009	0.002	0.002
s_5	(mm)	0.0	0.0	0.0	0.0
s_6	(mm)	46.7	44.515	46.291	47.736
α_1	(deg)	−90.0	−92.203	−92.523	−92.122
α_2	(deg)	−90.0	−87.816	−87.844	−88.446
α_3	(deg)	90.0	89.995	89.998	89.999
α_4	(deg)	0.0	0.000	0.001	0.000
α_5	(deg)	0.0	−0.001	0.000	0.000
α_6	(deg)	90.0	90.011	90.002	90.003
$\theta zero_1$	(deg)	0.000	0.006	0.002	0.001
$\theta zero_2$	(deg)	−90.000	−90.002	−90.001	−90.001
$\theta zero_3$	(deg)	36.087	38.069	36.111	36.009
$\theta zero_4$	(deg)	−80.654	−80.774	−79.742	−80.035
$\theta zero_5$	(deg)	45.996	44.212	45.063	45.181
$\theta zero_6$	(deg)	−135.000	−135.002	−135.000	−135.001
$\theta slope_1$	(deg/V)	16.0	15.908	15.825	15.716
$\theta slope_2$	(deg/V)	8.0	8.283	8.266	8.222
$\theta slope_3$	(deg/V)	8.0	6.064	7.857	7.770
$\theta slope_4$	(deg/V)	−16.0	−12.109	−15.876	−15.679
$\theta slope_5$	(deg/V)	−8.0	−6.125	−7.921	−7.842
$\theta slope_6$	(deg/V)	16.0	15.958	15.916	15.915
Device Parameters					
D_0	(mm)	0.0	−0.028	−0.008	−0.009
D_1	(mm)	110.0	110.0	110.0	110.0
D_2	(mm)	34.0	34.0	34.0	34.0
D_3	(mm)	134.0	134.0	134.0	134.0
D_4	(mm)	136.0	133.101	133.986	136.0
ψ	(deg)	0.0	−0.017	−0.004	−0.005

$n = 48$

Table 3 The effect of different ISL parameter sets on predicted and actual mean position residuals for the calibration positions and for noncalibration positions

| | ISL parameter set from Table 2 | | |
	B	C	D
Predicted calibration residuals			
flexion (deg)	0.465	0.499	0.477
abduction (deg)	0.317	0.342	0.353
tibial rotation (deg)	0.136	0.147	0.184
lateral translation (mm)	0.575	0.281	0.282
anterior drawer (mm)	0.236	0.292	0.298
joint distraction (mm)	0.670	1.207	1.210
Residuals for noncalibration positions			
flexion (deg)	0.078	0.147	0.147
abduction (deg)	2.304	0.388	0.405
tibial rotation (deg)	0.514	0.110	0.121
lateral translation (mm)	2.612	2.113	0.817
anterior drawer (mm)	1.166	0.168	0.523
joint distraction (mm)	4.529	0.921	0.889

$n = 48$

Initial mean position residuals averaged about eight degrees for the three rotational position parameters and 12 millimeters for the three translational position parameters. Convergence was typically attained in four iterations.

Column A of Table 2 lists the exact linkage and device parameters. To determine whether the simulated calibrations were a satisfactory representation of what is seen in practice, the same sets of ISL parameters were altered by the program. Column B, Table 2, shows the results when ISL parameters a_6, s_2, s_3, and s_5 were not altered (as in the actual run that resulted in the formation of the strange ISL parameter set listed in column B, Table 1). For the simulated calibration, the minimum number of calibration device parameters (D_1, D_2, and D_3) were held fixed to evaluate the ability of the program to calibrate the calibration device as well as the ISL. The resulting parameter set (column B, Table 2) shows the same trends as the set listed in column B, Table 1, which is based on actual data. For the calibration that produced column C, ISL parameter a_3 was additionally held fixed at its nominal value of zero millimeters. The resulting parameter set now is comparable to the true set—similar to what happened with the set from column C, Table 1. Noting that device parameter D_4 was not fit well in runs B or C, we held parameter D_4 at its true value of 136 millimeters for a final calibration; the output is listed in column D.

Satisfied that the simulated calibration was a satisfactory model of actual calibration, we compared the residuals produced by the three optimized ISL parameter sets over the 48 calibration positions and over twelve additional noncalibration positions consisting of permutations of 15, 45, and 75 degrees flexion, 10 and −10 degrees abduction, and 10 and −10 degrees tibial rotation. These non-calibration positions are well within the range of motion for a knee and the ISL should be accurate at these positions. Table 3 lists two different groups of residuals; (i) the mean residuals predicted by the calibration algorithm for the forty-eight calibration positions using the input voltage data with random error of $\pm 5 \times 10^{-2}$ Volts and (ii) the mean residuals for the twelve positions not part of the calibration.

Table 3 shows that the ISL parameter set listed in column B, Table 2, produced the lowest predicted residual set, but the

Table 4 For actual data, ISL calibration results and the predicted residuals when the minimum number of ISL and device parameters were held fixed. Those ISL and calibration device parameters accurate to only one digit after the decimal point have been held fixed.

ISL Parameters		Initial parameter set	$n=48$ Optimized parameter set
a_1	(mm)	0.0	-0.1484
a_2	(mm)	0.0	-0.2810
a_3	(mm)	0.0	0.0
a_4	(mm)	76.2	75.9119
a_5	(mm)	76.2	76.7245
a_6	(mm)	0.0	0.0
s_1	(mm)	33.0	33.8050
s_2	(mm)	0.0	0.0
s_3	(mm)	0.0	0.0
s_4	(mm)	0.0	-2.0973
s_5	(mm)	0.0	0.0
s_6	(mm)	46.7	46.2834
α_1	(deg)	-90.0	-90.7092
α_2	(deg)	-90.0	-89.7245
α_3	(deg)	90.0	90.1943
α_4	(deg)	0.0	0.0302
α_5	(deg)	0.0	0.1252
α_6	(deg)	90.0	90.3660
$\theta zero_1$	(deg)	-3.4	-4.2537
$\theta zero_2$	(deg)	-75.1	-75.9042
$\theta zero_3$	(deg)	8.5	4.4865
$\theta zero_4$	(deg)	-21.8	-19.6731
$\theta zero_5$	(deg)	15.9	12.6116
$\theta zero_6$	(deg)	-69.2	-68.9390
$\theta slope_1$	(deg/V)	8.0	7.8942
$\theta slope_2$	(deg/V)	8.0	8.1221
$\theta slope_3$	(deg/V)	8.0	8.8567
$\theta slope_4$	(deg/V)	-8.0	-8.0375
$\theta slope_5$	(deg/V)	-8.0	-8.6910
$\theta slope_6$	(deg/V)	16.0	17.5716
Device Parameters			
D_0	(mm)	0.0	0.1202
D_1	(mm)	110.0	110.0
D_2	(mm)	34.0	34.0
D_3	(mm)	134.0	134.0
D_4	(mm)	136.0	136.0
ψ	(deg)	0.0	0.0918
Mean Residuals			
flexion (deg)		6.074	0.500
abduction (deg)		1.525	0.296
tibial rotation (deg)		1.160	0.328
lateral translation (mm)		2.746	0.484
anterior drawer (mm)		2.391	0.718
joint distraction (mm)		4.009	0.793

non-calibration position residuals show that the strange ISL parameter set is inaccurate in measuring abduction, lateral translation, or joint distraction for noncalibration positions. For the ISL parameter set listed in Column C, Table 2, the second set of mean residuals show that the elimination of the interdependence involving ISL parameter a_3 has greatly improved the measurement of abduction and joint distraction for noncalibration positions. However, because of the difficulty in locating the correct value of D_4, this ISL parameter set is not accurate with lateral translation when used for noncalibration positions. Column D indicates that if device parameter D_4 can be accurately determined, the resulting ISL parameter set will be useful in measuring all six position parameters within the workspace of the knee.

Based on what was learned about parameter interdependence, a calibration on actual data was performed by holding fixed only the minimum set of ISL parameters (a_3, a_6, s_2, s_3 and s_5) and calibration device parameters (D_1, D_2, D_3, and D_4). The remaining twenty-seven parameters were refined by the algorithm. The results are presented in Table 4. The input data for this calibration was collected at a later date than that upon which Table 1 was based, and between calibrations the potentiometer gains and zeroes had been changed. For these data, the anatomical position parameters were weighted at

3000, and the calibration was completed in three iterations. The resulting residuals are roughly 0.4 degrees for the anatomical rotations and 0.7 millimeters for the anatomical translations. These values are in the range that was expected based upon the known resolution of the potentiometers and from the error analysis of this linkage design that was discussed in the companion paper [5].

In comparison with other calibration data found in the literature, Sommer and Miller [7] report achieving position residuals on the order of 0.5 degrees and 0.2 millimeters in the measurement of rotation and translation. Ahmed et al. [1] achieved measurement accuracy tolerances of 0.5 degrees and 0.5 millimeters. The residuals from our data are slightly larger, these being estimates of error in locating the moving bone with respect to the stationary bone when the ISL is in configurations as tested. This was accomplished by incorporating the **PRE** and **POST** matrix transformations into our optimization objective function. Even though transformations **PRE** and **POST** only approximate those corresponding to the anatomical joint, the accuracy estimates are still more informative that those obtained by other techniques. Because the purpose of the ISL is to measure bone motion and not linkage-end motion, the residuals from the objective function reported here are perhaps more realistic estimates for actual measurement error.
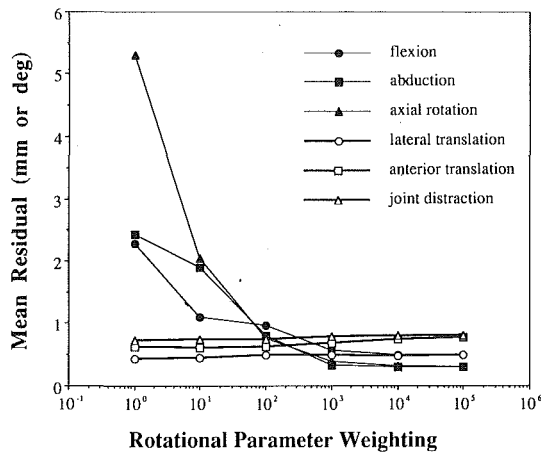
Fig. 4 Weighting the anatomical rotational position parameters in the calibration algorithm serves to greatly decrease rotational parameter mean residuals at the expense of a small increase in translational parameter mean residuals

Any function that uses different units—here length and angular dimensions—is weighted, whether planned or not. The objective function used by Sommer and Miller [7] used centimeters and radians as units of measure. This corresponds to a fixed rotational weight factor of 100 in the objective function used in this paper. Several optimizations were performed with the input data used in Table 2 to observe the effect of weighting on convergence and residuals. The rotational parameter weight factors were varied as a group while the translational parameter weight factors were maintained at unity. Program runs were performed for rotational parameter weight factors of 1, 10, 100, 1000, 10,000, and 100,000.

The overall effect of the weighting factors, as expected, is to control the distribution of measurement error among the six position parameters. As the rotational parameter weight factor increases, the rotational residuals decrease rapidly with a small increase in the translational residuals (Fig. 4). It was suggested earlier that if rotational accuracy of one degree is just as important as translational accuracy of one millimeter, a weight factor of 3000 would be near optimum. The residual curves in the figure appear to support this—therefore for general calibration use, a rotational weighting factor of 3000 is used as the standard weight factor.

Conclusion

The equation relating ISL voltages to anatomical joint position represents a theoretical model that simulates the actual ISL. Because this model and the actual ISL are not identical, a calibration scheme is necessary to get acceptable accuracy out of the ISL. The method of Sommer and Miller [7] is suitable for doing this, but there are potential problems with this method: (i) if the ISL is calibrated end-to-end rather than bone-to-bone, the resulting residuals cannot be taken as a measure of ISL accuracy in predicting bone position parameters; (ii) depending on ISL and calibration device design, calibration device degrees of freedom, and calibration positions, parameter interdependency can occur so that small residuals are attained; but the optimized ISL parameters are quite different from the actual parameters and large measurement error can occur for noncalibration device configurations; and (iii) the ISL will be best calibrated if the calibration space includes the anatomical workspace.

The calibration device and procedure we have developed reduces the magnitude of these problems by calibrating to known bone motions, as generated on a knee-like calibration device in which the known positions are located in terms of knee position parameter values, i.e. the device dials. By ex-

perimenting with the device and procedure, we have identified and eliminated interdependence of ISL and device parameters, forcing the calibration set to be similar to the actual values. This reduces the chance of large errors in noncalibration positions.

Although a six-DOF calibration device would be allow the capability to replicate any anatomical joint position and would eliminate some of the interdependent relationships between ISL and device parameters, we have found a four-DOF device satisfactory and its design and construction is considerably less complex than the required for a six-DOF calibration device.

From the experience gained as a result of the optimizations described in this paper:

(1) Calibrate the ISL in the same workspace in which the ISL is to be used. This means calibrate from "bone-to-bone," where the "bones" of the calibration device span the same space as those of the anatomical joint. This not only results in the creation of an optimized ISL parameter set that can be used with confidence, but through the residuals of the optimization ISL parameter set that can be used with confidence, but through the residuals of the optimization process, also allows for the evaluation of the accuracy of the ISL. In addition, A/D gains and potentiometer zeroes set for calibration can be used untouched in actual testing.

(2) Let as many ISL parameters as possible be adjusted by the program to converge to a reasonable parameter set that achieves the best residuals. To find the largest set of linkage parameters that do not have to be held fixed, an examination of interdependent parameter relationships is required. Observations of the physical geometry of the ISL will identify many of the interdependent relationships, but it is likely that trial-and-error will locate several more interdependent parameter relationships. Even though the optimized ISL parameter set is only a mathematical representation of the physical ISL, it should not differ greatly from the mechanically measured parameter set.

(3) The residual error for selected rotational and translational parameter can be lowered using weighting at the expense of error in the other rotational and translational parameters. We find that a rotational parameter weight factor that balances the linear units of millimeters and angular units of degrees is best for general calibration.

References

1 Ahmed, A. M., Hyder, A., Burke, D. L., and Chan, K. H., "In Vitro Ligament Tension Pattern in the Flexed Knee in Passive Loading," *Journal of Orthopaedic Research*, Vol. 5, 1987, pp. 217-230.

2 Grood, E. S., and Suntay, W. J., "A Joint Coordinate System for the Clinical Description of Three-Dimensional Motions: Application to the Knee," ASME JOURNAL OF BIOMECHANICAL ENGINEERING, Vol. 105, May 1983, pp. 136-144.

3 Kinzel, G. L., "On the Design of Instrumented Linkages for the Measurement of Relative Motion Between Two Rigid Bodies," Ph.D. dissertation, Purdue University, Lafayette, Ind., 1973.

4 Kinzel, G. L., and Hall, A. S., Jr., "Tolerances and Clearances in Instrumented Spatial Chains," *Proceedings of the Institution of Mechanical Engineers*, 1975, pp. 185-191.

5 Kirstukas, S. J., Lewis, J. L., and Erdman, A. G., "6R Instrumented Spatial Linkages for Anatomical Joint Motion Measurement—Part 1, Design," ASME JOURNAL OF BIOMECHANICAL ENGINEERING, published in this issue, pp.

6 Scales, L. E., *Introduction to Non-Linear Optimization*, Springer-Verlag, New York, 1987.

7 Sommer, H. J., and Miller, N. R., "A Technique for the Calibration of Instrumented Spatial Linkages Used for Biomechanical Kinematic Measurements," *Journal of Biomechanics*, Vol. 14, 1981, pp. 91-98.

8 Suntay, W. J., Grood, E. S., Hefzy, M. S., Butler, D. L., and Noyes, F. R., "Error Analysis of a System for Measuring Three-Dimensional Joint Mo-

tion," ASME JOURNAL OF BIOMECHANICAL ENGINEERING, Vol. 105, pp. 127–135.

9 Uicker, J. J., Jr., Denavit, J., and Hartenberg, R. S., "An Iterative Method for the Displacement Analysis of Spatial Mechanisms," ASME *Journal of Applied Mechanics*, Vol. 31, June 1964, pp. 309–314.

APPENDIX 1

The partial derivatives of the entries of **H** with respect to the adjustable ISL parameters are developed using a computationally efficient technique similar to that used by Uicker [9] in his solution of the spatial linkage inverse kinematics problem. As **H** is the product of the six $\mathbf{A}_i$ matrices, the derivatives of these matrices with respect to their constituents will be needed. The partial derivatives of the general $\mathbf{A}_i$ matrix with respect to a_i, s_i, α_i, $\theta slope_i$, and $\theta zero_i$ can be obtained by multiplying the $\mathbf{A}_i$ matrix by special derivative operator **Q** matrices. For the $\mathbf{A}_i$ matrix used in this paper, the **Q** matrices are as follows:

$$\mathbf{Q}_a = \begin{bmatrix} 0 & 0 & 0 & -1 \\ 0 & 0 & 0 & 0 \\ 0 & 0 & 0 & 0 \\ 0 & 0 & 0 & 0 \end{bmatrix} \quad (A.1a)$$

$$\mathbf{Q}_s = \begin{bmatrix} 0 & 0 & 0 & 0 \\ 0 & 0 & 0 & 0 \\ 0 & 0 & 0 & -1 \\ 0 & 0 & 0 & 0 \end{bmatrix} \quad (A.1b)$$

$$\mathbf{Q}_\alpha = \begin{bmatrix} 0 & 0 & 0 & 0 \\ 0 & 0 & 1 & 0 \\ 0 & -1 & 0 & 0 \\ 0 & 0 & 0 & 0 \end{bmatrix} \quad (A.1c)$$

$$\mathbf{Q}_\theta = \begin{bmatrix} 0 & 1 & 0 & 0 \\ -1 & 0 & 0 & 0 \\ 0 & 0 & 0 & 0 \\ 0 & 0 & 0 & 0 \end{bmatrix} \quad (A.1d)$$

The partial derivatives of $\mathbf{A}_i$ are as follows. Note that because matrix multiplication is not commutative, the multiplication order is critical.

$$\frac{\partial \mathbf{A}_i}{\partial a_i} = \mathbf{A}_i \mathbf{Q}_a \quad (A.2a)$$

$$\frac{\partial \mathbf{A}_i}{\partial s_i} = \mathbf{Q}_s \mathbf{A}_i \quad (A.2b)$$

$$\frac{\partial \mathbf{A}_i}{\partial \alpha_i} = \mathbf{A}_i \mathbf{Q}_\alpha \quad (A.2c)$$

$$\frac{\partial \mathbf{A}_i}{\partial \theta zero_i} = \mathbf{Q}_\theta \mathbf{A}_i \quad (A.2d)$$

$$\frac{\partial \mathbf{A}_i}{\partial \theta slope_i} = v_i \mathbf{Q}_\theta \mathbf{A}_i \quad (A.2e)$$

where:

The scalar quantity v_i is the voltage output of the ith potentiometer.

When the partial derivative of **H** with respect to one of the thirty adjustable ISL parameters is required, the appropriate **Q** matrix is inserted into the appropriate location in the matrix chain that develops **H**. For instance, to calculate the partial derivative of **H** with respect to s_3, $\mathbf{Q}_s$ is inserted in front of $\mathbf{A}_3$:

$$\frac{\partial \mathbf{H}}{\partial s_3} = \mathbf{D}(s_3) = [\mathbf{PRE}][\mathbf{A}_6 \, \mathbf{A}_5 \, \mathbf{A}_4 \, \mathbf{Q}_s \, \mathbf{A}_3 \, \mathbf{A}_2 \, \mathbf{A}_1] \, [\mathbf{POST}]. \quad (A.3)$$

The partial derivative of **H** with respect to s_3 is represented as matrix $\mathbf{D}(s_3)$. The matrix product $(\mathbf{A}_6\mathbf{A}_5\mathbf{A}_4)^{-1}(\mathbf{A}_6\mathbf{A}_5\mathbf{A}_4)$, equivalent to the identity matrix, can be inserted into the above equation following the **Q** matrix. After linear algebra manipulation, the result is:

$$\frac{\partial \mathbf{H}}{\partial s_3} = \mathbf{D}(s_3) = [\mathbf{PRE}][(\mathbf{A}_6 \, \mathbf{A}_5 \, \mathbf{A}_4)\mathbf{Q}_s \, (\mathbf{A}_6 \, \mathbf{A}_5 \, \mathbf{A}_4)^{-1}\mathbf{H}_{\mathrm{ISL}}][\mathbf{POST}].$$

$$(A.4)$$

The partial derivatives of **H** with respect to any of the other 29 ISL parameters are obtained similarly.

APPENDIX 2

The following outlines the Levenberg-Marquardt method, which is covered in more detail in the book by Scales [6]. Letting **x** be the vector of estimates for the thirty ISL parameters and six calibration device parameters, then the weighted objective function is: $F(\mathbf{x}) = \Sigma w_i \{v_i(\mathbf{x})\}^2$. In this equation, v_i are the components of **v**, the vector of differences between known position parameters and calculated position parameters. There is one term for each of the six anatomical position parameters at the n calibration positions, for a total of $6n$ terms. Weighting capability is provided with the w_i terms. In matrix notation, the function becomes: $F(\mathbf{x}) = \mathbf{v}^T\mathbf{w}\mathbf{v}$, where **w** is a $(6n) \times (6n)$ weight factor matrix. The Jacobian matrix of first partial derivatives, **J** is used to lead to a lower objective function value. For the calibration problem, this matrix has $6n$ rows, each corresponding to one of the six anatomical position parameters at the n calibration positions, and up to thirty-six columns, one column for each linkage or calibration device parameter.

Now for the form of the Levenberg-Marquardt algorithm used in ISL calibration:

Levenberg-Marquardt Algorithm

Given: the six accurately known position parameters corresponding to each of the n calibration positions (the settings of the calibration device), n sets of six voltages from the ISL potentiometers, and $\mathbf{x}_0$, the vector of initial estimates for the thirty ISL parameters and six calibration device parameters.

- set μ at 0.01, ν at 10, and gtol to 1.5.
- Evaluate difference vector $\mathbf{v}_0$.
- Evaluate initial weighted objective function: $F_0 = [\mathbf{v}_0]^T\mathbf{w}[\mathbf{v}_0]$.
- For $m = 0, 1, 2\ldots$ repeat
  - decrease μ: $\mu = \mu/\nu$.
  - repeat
    - Using Gaussian elimination with total pivoting, solve for vector **p** in the matrix equation: $([\mathbf{J}_m]^T\mathbf{w}[\mathbf{J}_m] + \mu\mathbf{I})\mathbf{p} = [\mathbf{J}_m]^T\mathbf{w}\mathbf{v}_m$.
    - Update estimates of the adjustable parameters: $\mathbf{x}_{m+1} = \mathbf{x}_m + \mathbf{p}$.
    - Evaluate difference vector $\mathbf{v}_{m+1}$.
    - Evaluate weighted objective function: $F_{m+1} = [\mathbf{v}_{m+1}]^T\mathbf{w}[\mathbf{v}_{m+1}]$.
    - If $F_{m+1} > F_m$, then increase μ: $\mu = \mu\nu$.
  - end when $F_{m+1} < F_m$.
- End when $\|2[\mathbf{J}_{m+1}]^T\mathbf{w}[\mathbf{v}_{m+1}]\| <$ gtol.